

## Ferroelectric Nanocomposite Networks with High Energy Storage Capacitance and Low Ferroelectric Loss by Designing Hierarchical Interface Architecture

Yingxin Chen,<sup>a</sup> Yifeng Yue,<sup>a</sup> Jie Liu,<sup>c</sup> Jie Shu,<sup>e</sup> Aiping Liu,<sup>d</sup> Baojin Chu,<sup>c</sup> Minhui Xu,<sup>a</sup> Weizhong Xu,<sup>d</sup> Tong Chen,<sup>a</sup> Jian Zhang<sup>a\*</sup>, Qundong Shen<sup>b\*</sup>

a. College of Materials & Environmental Engineering, Hangzhou Dianzi University, Hangzhou 310018, China.

b. Key Laboratory of High Performance Polymer Materials and Technology of MOE, School of Chemistry & Chemical Engineering, Nanjing University, Nanjing, 210023, China

c. CAS Key Laboratory of Materials for Energy Conversion and Department of Materials Science and Engineering, University of Science and Technology of China, No. 96 Jinzhai Rd., Hefei, Anhui, 230026, China

d. Center for Optoelectronics Materials and Devices, Zhejiang Sci-Tech University, Hangzhou, 310018, China.

e. Analysis and Testing Center, Soochow University, Suzhou, 215123, China.

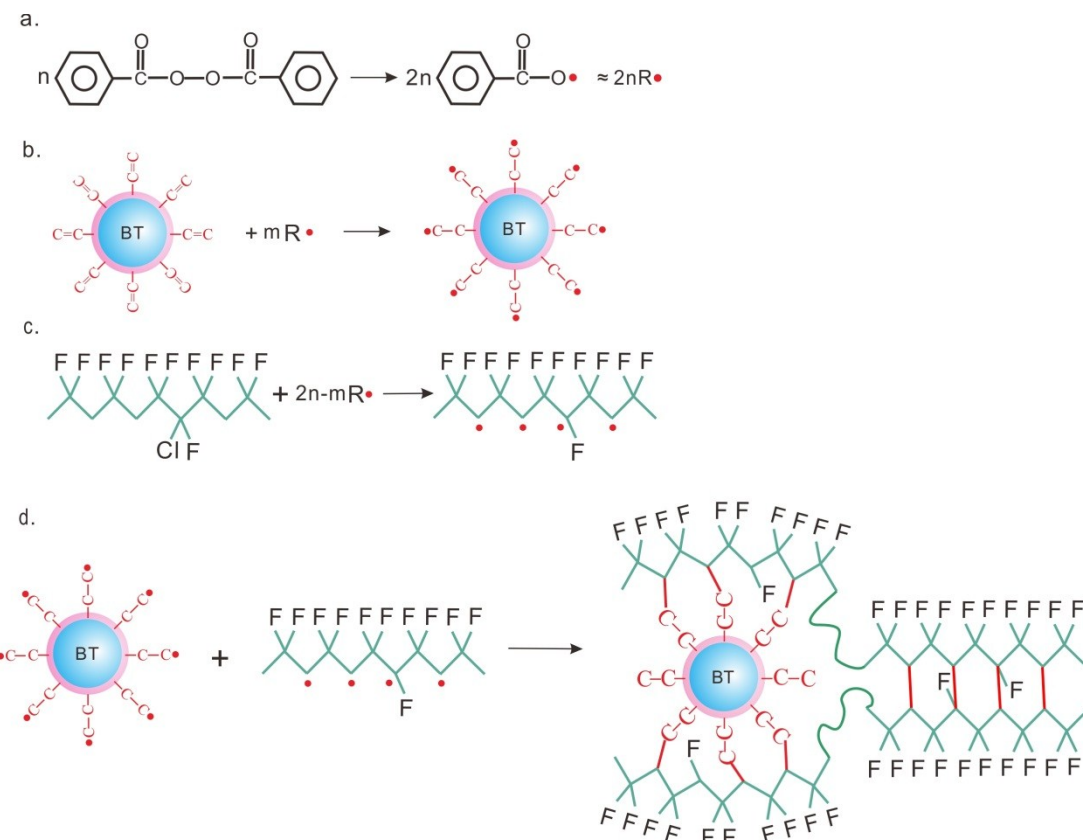


Figure S1. Schematic illustration of the mechanism of the cross-linking reactions in P(VDF-CTFE)/MPS@BT nanocomposite networks.

Table S1. Lattice constant and coherence length for the (200, 020) reflection of P(VDF-CTFE)/MPS@BT nanocomposites ( $B_0$ ,  $B_5$ ,  $B_{10}$ , and  $B_{15}$ ) and nanocomposite networks ( $B_{10}P_{10}$ , and  $B_{10}P_{15}$ ).

	$\alpha$ -phase		$\beta$ -phase	
	$d$ , Å (020)	$L$ , nm	$D$ , Å(100, 200)	$L$ , nm
P(VDF-CTFE)	4.48	11.0	4.32	6.7
$B_5$	4.43	10.3	4.28	7.3
$B_{10}$	4.46	9.7	4.30	8.1
$B_{15}$	4.45	8.1	4.29	9.0
$B_{10}P_{10}$	4.43	7.3	4.31	6.2
$B_{10}P_{15}$	4.46	6.5	4.31	5.8

Table S2. Melting temperature ( $T$ ) and the relative crystallinity of the P(VDF-CTFE)/MPS@BT nanocomposites and nanocomposite networks calculated from DSC curves.

Sample	$T_m$ (°C)	Crystallinity (%)
P(VDF-CTFE)	173	23.6
$B_5$	171	25.2
$B_{10}$	172	25.4
$B_{15}$	171	26.1
$B_{10}P_{10}$	169	22.4
$B_{10}P_{15}$	168	21.7

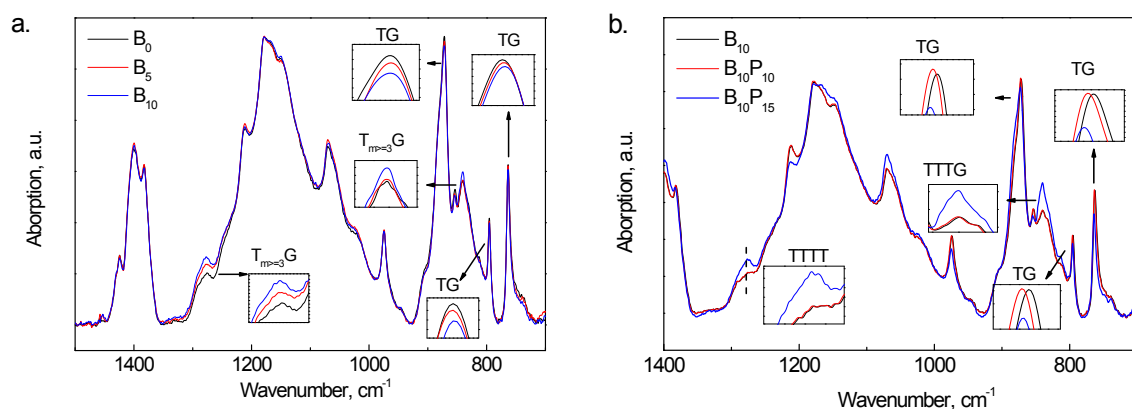


Figure S2. FTIR spectrum of (a) P(VDF-CTFE) and P(VDF-CTFE)/MPS@BT nanocomposites ( $B_5$ , and  $B_{10}$ ).

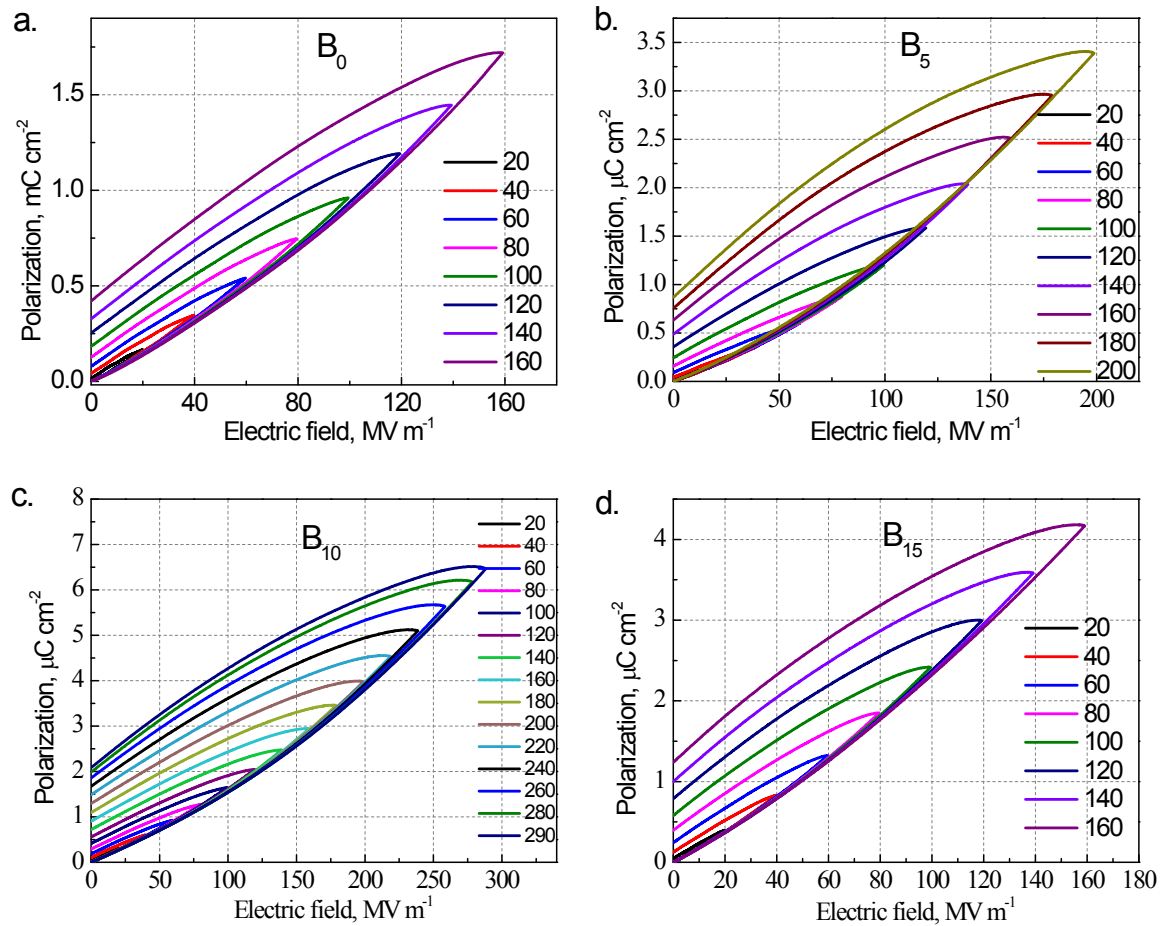


Figure S3. Unipolar D-E hysteresis loops for P(VDF-CTFE)/MPS@BT nanocomposites (a)  $B_0$ , (b)  $B_5$ , (c)  $B_{10}$ , and (d)  $B_{15}$ .

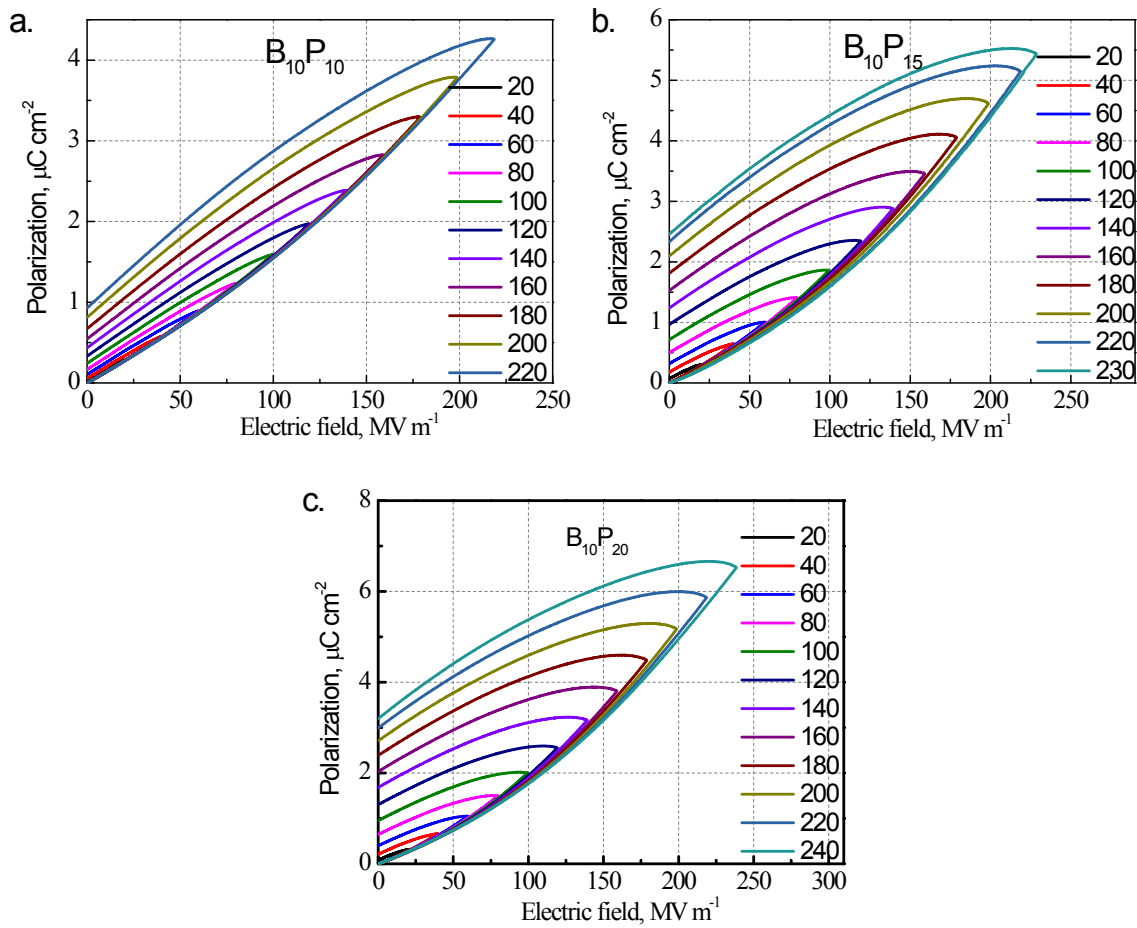


Figure S4. Unipolar D-E hysteresis loops for P(VDF-CTFE)/MPS@BT nanocomposite networks (a)  $B_{10}P_{10}$ , (b)  $B_{10}P_{15}$ , and (c)  $B_{10}P_{20}$ .